Improved real-time bio-aerosol classification using Artificial Neural Networks

Maciej Leśkiewicz[1], *Miron Kaliszewski[2], Maksymilian Włodarski[2], Jarosław Młyńczak[2], Zygmunt Mierczyk[2], Krzysztof Kopczyński[2].

1. PCO S.A. ul. Jana Nowaka-Jeziorańskiego 28, 03-982 Warsaw, Poland.
2. Institute of Optoelectronics, Military University of Technology, ul. Gen. Witolda Urbanowicza 2, 00-908 Warsaw, Poland

*Corresponding author: miron.kaliszewski@wat.edu.pl

Keywords: Bio-aerosol, Fluorescence, Real-time analysis, Artificial Neural Network, PBAP.

1. Abstract

Air contamination has had stronger and stronger impact on everyday life of humans. An increasing number of people are aware of the health problems that may result from inhaling air which contains dust, bacteria, pollens or fungi. There is a need for real-time information about ambient particulate matter. The devices, currently available on the market, can to detect some particles in the air, but cannot classify them by the health threats. Fortunately, a new type of technology is emerging as a promising solution.

Laser based bio-detectors are opening a new era in aerosol research. They are capable of characterizing a great number of individual particles in seconds by analyzing optical scattering and fluorescence characteristics. In this study we demonstrate application of Artificial Neural Network (ANN) to real-time analysis of single particle fluorescence fingerprints acquired using BARDet (Bio-aerosol detector). The 48 different aerosols including pollens, bacteria, fungi, spores, and non-biological substances were characterized. An entirely new approach to data analysis using decision tree comprising 22 independent neural networks was discussed. Applying confusion matrices and ROC analysis the best sets of ANN's for each group of similar aerosols has been determined. As a result an impressive effectiveness of aerosol classification in real-time was achieved. It was found that for some substances that have characteristic spectra almost each particle can be properly classified. The aerosols with similar spectral characteristics can be classified as a specific cloud with high probability. In both cases the system recognized aerosol type with no mistake.

2. Introduction

The ambient air contains a variety of particles like dust, bacteria, pollens, fungi and other parts of biological and non-biological origin(Pöhlker et al., 2013; Górny, 2004). The aerosols are involved in various atmospheric processes like ice nuclei formation, precipitation and global climate effects (Deguillaume et al., 2008; Fröhlich-Nowoisky et al., 2016; Gabey et al., 2010; Pósfai and Buseck, 2010; Fuzzi et al., 2015). They also strongly influence human health (Davidson et al., 2005; Pope III and Dockery, 2006; Michaels, 2017; Shiraiwa et al., 2012). Therefore, the characterization of ambient air is important for estimating potential health hazards and environmental impact (Mauderly and Chow, 2008; Lim et al., 2005). Standard methods of aerosol composition assessment usually include microscopic inspection or molecular analysis of filter (Miaskiewicz-Peska and Lebkowska, 2012), tape or liquid trapped particles. Nevertheless, they suffer from low time resolution due to periodical and relatively long analytical procedures. They are also ineffective for the detection of non-culturable

Deleted: containing

Deleted: Society is awaiting anxiously for a system that could inform them in real-time about a real danger that is suspended in the air… The devices, currently available on the market, are able…an to detect some particles in the air, but cannot classify them by the health threats. Fortunately, a new type of technology is emerging as a really …

Deleted: We gathered a total of 114779 spectra…he of…48 different aerosols including pollens, bacteria, fungi, spores, and non-biological substances were characterized. We discuss a …

Deleted:

Deleted: we …n impressive achieved very high performance effectiveness of aerosol classification in real-time was achieved. V …

Deleted:)

Formatted: German (Germany)

Field Code Changed

Deleted: (

Field Code Changed

Formatted: German (Germany)

Formatted …

Deleted:

Formatted: German (Germany)

Field Code Changed

Deleted:)

Deleted: (

Formatted: German (Germany)

Deleted:)

Formatted …

Field Code Changed

Deleted: (

Formatted: German (Germany)

Formatted: German (Germany)

Deleted:)

Deleted: (

Formatted: German (Germany)

Field Code Changed

Field Code Changed

Deleted:)

Field Code Changed

Deleted: (…uzzi et al., 2015). They also strongly influence human health (Davidson et al., 2005;)… (…ope III and Dockery, 2006;)… (…ichaels, 2017;)… (…

Formatted …

Deleted:)… (…

microorganisms (Blais-Lecours et al., 2015; Trafny et al., 2014).

The detection and classification of biological particles is possible using fluorescence techniques due to the presence of proteins, NADH, and some vitamins that emit light when excited with UV light (Lakowicz, 1999). This feature is utilized in single particle fluorescence detectors. In the flowing air each particle is characterized for size/shape using light scattering as well as fluorescence properties. This approach ensures continuous measurement and immediate response. Thus the analysis process can be facilitated and accelerated compared with other commonly used analytical procedures (Hill et al., 1999; Choi et al., 2014; Taketani et al., 2013; Feugnet et al., 2008).

Several studies using single particle fluorescence detectors demonstrated that fluctuations of aerosol concentration and variations in its fluorescence properties are strongly dependent on the season, day time, location and a place occupancy (Gabey et al., 2011; Huffman et al., 2010; Pinnick et al., 2004; Bhangar et al., 2014; Fennelly et al., 2018). Each single particle passing the instrument is labelled with the time, scattering properties (size and/or shape) and fluorescence characteristics. It is obvious that continuous single particle measurements bring a new potential and quality to environmental research. However, particles of the same type and batch display slightly different spectral characteristics due to variations in biochemical composition, size, age in a population (Agranovski et al., 2003), degradation or stress level (Lee et al., 2010) and the particle position within instrument's interrogation point (Pan et al., 2011). The simple statistics, like data averaging and graphical spectra representation, are not sufficient. Therefore, the huge amount of data and occurring spectral variations require more advanced algorithms supporting automatic data classification. Various analytical methods of particle discrimination and classification were applied. It has been shown that Principal Component Analysis (PCA), Linear Discriminant Analysis (LDA), Hierarchical cluster Analysis (HCA) of fluorescence spectra strongly increases discrimination of particles compared with methods based on spectra averaging or fluorescence threshold (Leśkiewicz et al., 2016; Kaliszewski et al., 2013; Pan et al., 2012; Hernandez et al., 2016). Artificial neural network (ANN) is an emerging analytical approach that becomes more widely and successfully applied in various life domains like chemical analysis (Borecki et al., 2008), image recognition (Antowiak and Chałasińska-Macukow, 2003), data mining and weather forecasting (Purnomo et al., 2017). It has been shown that ANN can be applied in bio-aerosol classification (Kohlus and Bottlinger, 1993). However, it usually requires more user input comparing to other analytical procedures (Ruske et al., 2017).

This paper focuses on the application of ANN for real time discrimination of bio-aerosols based on single particle fluorescence characteristics. We demonstrated a new approach to data analysis using ANN allowing automatization of data preparation procedures and minimum user involvement.

3. Materials and methods

3.1. Experiment

3.1.1. BioAeRosol Detector (BARDet)

The detailed information concerning construction and parameters of the instrument used for the experiments was presented in our previous work (Kaliszewski et al., 2016). In general, the ambient air is continuously drawn through the nozzle. It is focused with sheath flow of filtered air. Particles in the focused air pass through the BARDet's chamber where they are interrogated by a 16mW CW laser beam generated by a diode laser operating at 375 nm wavelength (CUBE, Coherent). The backward and forward scattered signals are detected with two PMT's (H6780, Hamamatsu) mounted at the 35°and 145° angle to the laser beam axis.

Deleted:)
Deleted: (
Deleted:)
Deleted: (
Deleted:)
Deleted: (
Deleted:)
Deleted: (
Deleted:)
Deleted: (
Deleted:)
Deleted: (
Deleted:)
Deleted: (
Deleted:)
Deleted: (
Deleted:)
Deleted: (
Field Code Changed
Formatted: German (Germany)
Formatted: German (Germany)
Formatted: German (Germany)
Field Code Changed
Formatted: German (Germany)
Formatted: German (Germany)
Formatted: German (Germany)
Field Code Changed
Deleted: basing

The fluorescence of particles is measured at a 90° angle to the laser beam with 32 channel PMT (A10766, Hamamatsu). The longpass filter with cutting edge at 400 nm (Edmund Optics) separates the fluorescence signal from scattered light. The multichannel PMT measures fluorescence in 18 active channels in the range of 415.4-643.5 nm. The channels are grouped in 7 bands. The remaining channels are not used. The band configuration is presented in Table 1.

Table 1. Configuration of bands in the multichannel PMT.

BARDet's Fluorescence Bands	Bandwidth [nm]
B1	415.4 – 429.3
B2	443.1 – 456.8
B3	470.5 – 484.2
B4	497.8 – 524.9
B5	538.3 – 565.0
B6	578.3 – 604.6
B7	617.6 – 643.5

3.1.2. Aerosols

Deleted: Biological

Deleted: purpose of

For the tests, dry powders of harmless substances were used, since they did not need a specialized aerosol protection chamber. In order to achieve reliable aerosol classification the ANN's needs to be trained using possibly large number of measurement data. Therefore, various particle types, that can be easily aerosolized, were tested. Samples like pollens, fungi, bacteria, spores and leaves scraps naturally occur in the atmosphere. Biofluororphores like riboflavin, cellulose, aminoacids and proteins were also characterized since they are present in biological materials. The group of bacterial growth media was investigated due to their strong influence on bacteria fluorescence especially if they are not sufficiently washed. This can occur in case of intentionally released bacterial aerosols. Due to technical limitations the other than pharmaceutical samples could be aerosolized in this study. The aerosols of flours, and fluorescent non-biological substances like paper dust, AC fine Test Dust and talc were analyzed since they can occur especially in indoor and public places. The non-fluorescent particles were not a subject of the research since they can be automatically discarded as non-biological applying given fluorescence threshold.

The samples used for this study are listed in Table 2. To perform numerous experiments, disposable vials were used, one for each aerosol sample. It prevented cross contamination between measured samples. The aerosols were generated from modified 50 ml Falcon tubes placed on the vortex. The vials in the lower part contained two connectors for silicon tubes. Vortexed particles were entrained and formed an aerosol cloud inside the Falcon tube. The aerosolized particles were aspirated from the vial to BARDet's aerosol inlet. Each tube contained about 50 mg of the dry powder sample. During aerosol generation filtered air was supplied into the vial to compensate the BARDet's flow. The concentration of the aerosols was adjusted with vibration frequency of the vortex. The measurement started after the aerosol reached homogeneous concentration. The

experimental setup is shown in figure 1.

Table 2. List of all substances used in experiment.

	Abbreviation	Name	Size	AF	Source	Group
1	FM7	Fluoromax microspheres 7 um	6,25±0,91	0,92±0,02	Thermo scientific	standard 1
2	Rib	Riboflavin	2,22±1,82	0,88±0,09	Sigma-Aldrich	standard 2
3	BGP	Bermuda grass pollen	28,35±0,6	0,97±0,01	Duke Sci. Corp.	
4	CP	Corn pollen	78,13±1,22	0,95±0,01	Duke Sci. Corp.	
5	CA	*Corylus avellana* pollen	27,71±1,33	0,67±0,04	(*OC)	
6	LP	*Lycopodium* pollen	30,67±1,2	0,94±0,01	Fluka	
7	PPP	*Poa pratrensis* pollen	30,62±0,87	0,94±0,01	Sigma-Aldrich	
8	RP	Ragweed pollen	19,48±0,78	0,99±0,01	Duke Sci. Corp.	
9	SCP	*Secale cereale* pollen	44,8±2,01	0,94±0,01	Sigma-Aldrich	
10	SP	Spruce pollen	70,09±4,16	0,88±0,02	(*OC)	
11	AA	*Abies alba* pollen	84,56±12,77	0,92±0,02	(*OC)	
12	UDP	*Urtica dioica* pollen	14,99±1,26	0,9±0,05	(*OC)	pollens
13	PSP	*Pinus sylvestris* pollen	39,29±1,44	0,93±0,02	(*OC)	
14	PNP	*Pinus nigra* pollen	44,97±1,33	0,88±0,03	(*OC)	
15	LPP	*Lycopodium* pollen (Poland)	28,66±0,6	0,95±0,01	(*OC)	
16	PMP	Paper mulberry pollen	13,57±0,88	0,94±0,04	Duke Sci. Corp.	
17	ATP	*Artemisia tridentata* pollen	22,53±0,42	0,96±0,01	Sigma-Aldrich	
18	AAP	*Artemisia absynthium* pollen	18,37±1,51	0,96±0,02	Sigma-Aldrich	
19	CPP	*Chenopodium* pollen	27,29±0,97	0,98±0,01	(*OC)	
20	BWF	Buck wheat flour	25,17±15,76	0,82±0,06	MELVIT Poland (*RS)	
21	PF	Potato flour	21,23±3,11	0,96±0,03	KUPIEC Poland (*RS)	
22	RF	Rice flour	18,22±6,23	0,6±0,07	MELVIT Poland (*RS)	flours
23	TF	Tapioca flour	12,91±3,41	0,7±0,06	COCK BRAND (*RS)	
24	WF	Wheat flour	20,57±4,36	0,62±0,07	MELVIT Poland (*RS)	
25	Trp	Tryptophan	15,42±8,96	0,81±0,08	Sigma-Aldrich	
26	Phe	Phenylalanine	10,41±5,31	0,73±0,11	Sigma-Aldrich	
27	BSA	Bovine Serum Albumin	63,8±30,49	0,43±0,05	POCH Poland	amino acids and proteins
28	OVA	Ovalbumin	26,45±5,31	0,83±0,07	POCH Poland	
29	Ambio	*Bif. animalis, S. boulardii, S. thermophilus, L. casei, L. bulgaricus*	27,97±4,42	0,84±0,03	AMBIO Probiotyk, Lab. Galenowe Poland (*P)	bacteria in medium
30	LCB	*Lactobacillus bulgaricus*	51,16±19,33	0,68±0,08	LakciBios, ASA Poland (*P)	bacteria in medium

Deleted: Own collection
Deleted: on
Deleted: Own collection
Deleted: Own collection
Deleted: Own collection
Deleted: Own collection
Deleted: Own collection
Deleted: Own collection
Deleted: Regular shop
Deleted: Regular shop
Deleted: Regular shop
Deleted: Regular shop
Formatted: Polish
Formatted: Polish
Deleted: Pharmacy
Deleted: Pharmacy

31	LF	*Bifidobacterium animalis, L. acidophilus*	32,62±8,45	0,82±0,07	Linex forte, LEK Pharmaceuticals d.d. Slovenia (*P)	
32	BA	Bacteriological Agar	49,47±10,03	0,74±0,07	Sigma-Aldrich	medium
33	BAB	Blood Agar Base	18,78±2,11	0,71±0,12	Sigma-Aldrich	
34	LB	Luria broth	15,11±6	0,67±0,07	Sigma-Aldrich	
35	NB	Nutrient broth	42,67±9,21	0,69±0,03	Sigma-Aldrich	
36	BTSTG	*Bacillus thuringiensis* spores technical grade	7,13±5,95	0,72±0,12	Agricultural	Bacterial spore with admixtures
37	SB	*Saccharomyces boulardii*	57,82±7,56	0,69±0,05	Enterol, Biocodex France (*P)	funghi with admixtures
38	SC	*Saccharomyces cerevisiae*	21,33±5,55	0,76±0,07	Dr. Oetker Germany (*RS)	
39	LS	*Lycoperdon* spores	14,52±0,62	0,92±0,02	(*OC)	fungal spores
40	JGSS	Johnsons grass smut spores	6,91±0,34	0,98±0,02	Duke Sci. Corp.	smut spore (fungal spore)
41	BGSS	Bermuda grass smut spores	6,47±0,27	0,97±0,02	Duke Sci. Corp.	
42	ACFTD	AC Fine Test Dust	3,47±2,34	0,87±0,09	Duke Sci. Corp.	
43	NT	Nivea talc	14,33±4,71	0,77±0,09	Nivea Baby (*RS)	
44	PPD	Printer paper dust	76,37±18,89	0,43±0,11	XEROX Laserprint collected from paper shredder (*RS)	
45	PTD	Paper towel dust	73,45±25,65	0,56±0,15	Merida Poland collected from crushed towel (*RS)	other
46	Cin	Cinnamon	23,97±4,39	0,78±0,05	Kamis Poland (*RS)	
47	Cel	Celulose	82,86±14,28	0,25±0,04	Sigma-Aldrich	
48	GGL	Ground Green Leaves	18,03±4,3	0,77±0,09	Dried and ground Oak (*OC)	

*OC – pollens collected from trees, flowers and grass at the region of Warsaw during vegetative seasons in 2015 and 2016.

*RS – Regular shops in Warsaw where common goods are purchased.

*P – Pharmacy shops in Warsaw

Deleted: Pharmacy

Deleted: Pharmacy

Deleted: Regular shop

Deleted: Own collection

Deleted: Regular shop

Formatted: Font: (Default) Calibri, Font color: Black, English (United States)

Deleted: Regular shop

Deleted: Regular shop

Deleted: Regular shop

Deleted: Grinded

Deleted: Own collection

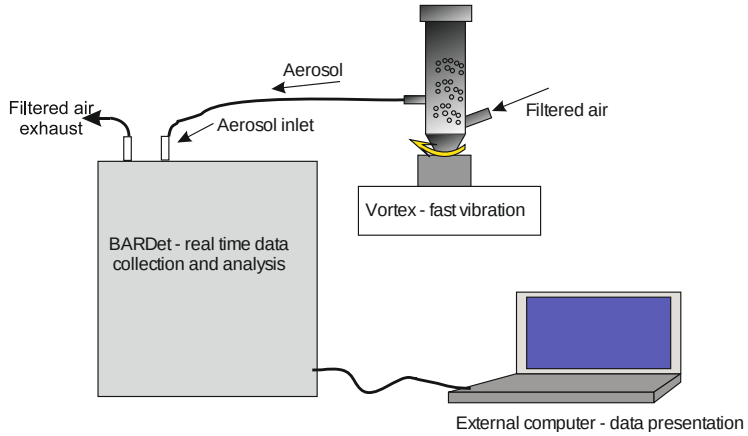

Figure 1. Setup of aerosol generation, data recording and analysis.

3.1.3. Aerosol microscopy

For microscopy analysis the aerosols were generated as described above and collected by impaction on a glass microscopic slide. The visualization of the samples was performed using Nikon Eclipse Ti-U microscope with 10x objective. The images were recorded with 5 megapixel DS-Fi1 camera. The aerosol equivalent diameters and circularity were analyzed automatically using NIS-Elements 64bit 3.22.10 software. The threshold of particles outline was corrected manually to obtain visually best fit.

3.1.4. Data acquisition method and pre-processing

The fluorescence of each particle was recorded in 7 bands. It creates a time series of the signals which has to be pre-processed before further analysis. There are two steps of gathering data. First one is performed by internal BARDet's software, which is responsible for controlling the instrument and the acquisition of raw signals. Then data is forwarded to a pre-processing module of analysis software. Its first task is to extract valuable signals from the noise (three sigma rule). Then a normalization procedure is required. It is realized first by subtracting the average value of signal and then it normalizing to its standard deviation. The main goal was to analyze shape of emission spectrum (not signal strength). An exemplary visualization of input data is shown in figure 2.

The data acquisition process started after stabilization of aerosol generation rate which was measured by the device. It was important to not exceed one particle per 2 ms of data integration time at 20 us measurement window. Finally, it was gathered a total of 114 779 spectral characteristics of 48 aerosols which gives in average almost 2400 fluorescence characteristics per substance.

Formatted: Font: Not Bold
Formatted: Font: Not Bold
Formatted: Standard, Indent: First line: 0,75 cm, Add space between paragraphs of the same style, No bullets or numbering
Formatted: Font: Not Bold
Formatted: Font: Not Bold
Formatted: Font: Not Bold, Font color: Auto
Formatted: Font: Not Bold
Formatted: Font: Not Bold
Formatted: Font: Not Bold
Formatted: Font: Not Bold
Formatted: Indent: Hanging: 0,89 cm, Outline numbered + Level: 3 + Numbering Style: 1, 2, 3, … + Start at: 1 + Alignment: Left + Aligned at: 3,43 cm + Indent at: 2,16 cm

Deleted: An Important aspect of t
Deleted: was monitoring the rate of generation of aerosol, which should be stable (not too high or spontaneous).
Deleted: we
Deleted: signals
Deleted: It is important to note that fact because of its statistical value for the further analysis.

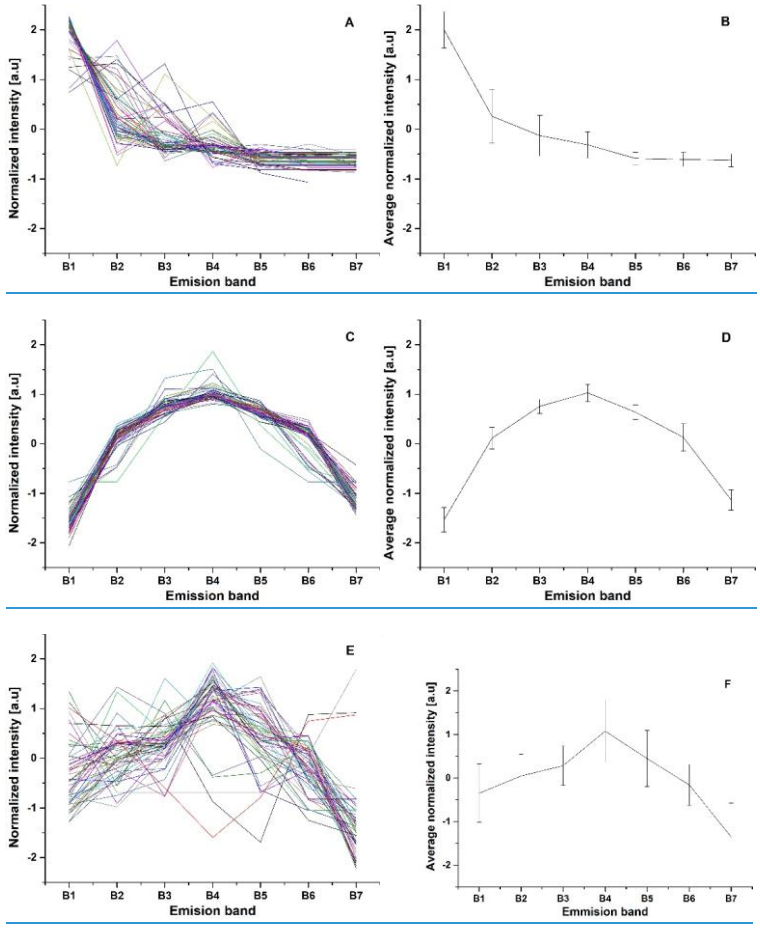

Figure 2. Normalized 50 subsequent fluorescence characteristics of NT (A), FM7 (C) and LCB (E) and corresponding averaged normalized intensities of NT (B), FM7 (D) and LCB (F). Error bars represent standard deviation of measurements.

3.2. Data analysis

3.2.1. ANN (Artificial Neural Network)

3.2.1.1. Basics

There are many types of Artificial Neural Networks (ANN), but in this paper only the backpropagation algorithm is demonstrated because it is one of the most practical ones. The main concept of this algorithm is based on a model of neuron that has two tasks. It aggregates signals (1) and then processes them by an activation function (2), which, in this research, is a sigmoid. The result of such single processing is a new signal z_j propagated to other neurons (Figure 3).

Formatted: Outline numbered + Level: 2 + Numbering Style: 1, 2, 3, … + Start at: 2 + Alignment: Left + Aligned at: 2,03 cm + Indent at: 1,4 cm

Formatted: Indent: Hanging: 0,89 cm, Outline numbered + Level: 3 + Numbering Style: 1, 2, 3, … + Start at: 1 + Alignment: Left + Aligned at: 3,43 cm + Indent at: 2,16 cm

Formatted: Indent: Hanging: 1,14 cm, Outline numbered + Level: 4 + Numbering Style: 1, 2, 3, … + Start at: 1 + Alignment: Left + Aligned at: 4,95 cm + Indent at: 3,05 cm

Deleted: 2

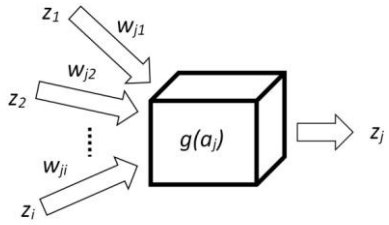

Figure 3. Mathematical model of single neuron cell.

Deleted: 2

$$a_j = \sum_i w_{ji} z_i \tag{1}$$

a_j- aggregated signal, w_{ji}- weight that connects neuron *i* with *j*, z_i- signal (input).

$$g(a_j) = \frac{1}{1 + e^{-\beta a_j}} \tag{2}$$

$g(a_j)$ – sigmoidal function, β- parameter (steepness) of sigmoid curve.

The structure of neural network is formed by layers of neurons: input, hidden and output. In this research input neurons are fluorescence spectrum and output neurons represent substances. In hidden layers (one and two hidden layers were examined) mostly actual computations are done. The schematic representation of neuron layers is presented in Figure 4.

Deleted: 3

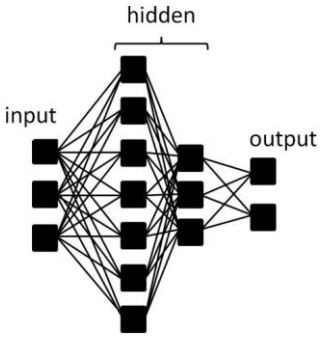

Figure 4. Typical topology of artificial neural network.

Deleted: 3

The described algorithm is the supervised learning method that requires training data for a teaching process. This allows one to calculate an error between the showed target and the ANN response. Every problem is related to minimizing output error which is calculated as Mean Squared Error (3).

$$E = \frac{1}{2}\sum_{k=1}^{c}(y_k - t_k)^2 \quad (3)$$

E – Mean Squared Error, t_k- observed value (target), y_k- calculated response, k-output neuron, c – number of output neurons.

Gradient descent method is used to find a minimum of error function. Error is dependent on network weights Δw_{ji} which might be adjusted (4). In order to update weights correctly, the first one needs to propagate error backward by calculating partial derivatives δ_j (5) (Figure 5). All mathematical details are well described by Ch. M. Bishop book (Bishop, 1995).

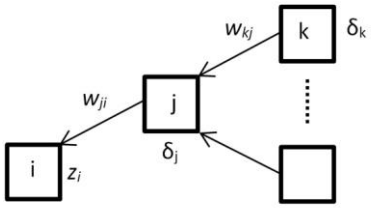

Figure 5. Model of backward error propagation.

$$\Delta w_{ji}(t) = -\eta\delta_j z_i + m\Delta w_{ji}(t-1) \quad (4)$$

η- learning rate, m - momentum, t - iteration.

$$\frac{\delta E}{\delta w_{ji}} = \frac{\delta E}{\delta a_j}\frac{\delta a_j}{\delta w_{ji}} = \delta_j z_i \qquad \delta_j = g'(a_j)\sum_k w_{kj}\delta_k \quad (5)$$

The learning rate factor determines the size of the steps while momentum parameter helps to skip local minimum by adding a fraction of the weight correction from the last step.

After the correction of all weights of ANN, the output error is examined and the procedure starts again unless an error level is low enough and there is no overfitting. All data are divided into three different sets: training, test and validation. For calculations during the learning process, only the first two are used. In order to determine whether it is time to stop teaching process, one has to observe an error in the test set. There will be a moment when this error comes to be constant or starts increasing due to the overfitting of training data (Figure 6). The validation data set may be useful for confronting different models or just to verify the current model on completely separate set of data.

Deleted: 4

Deleted: 4

Deleted: 5

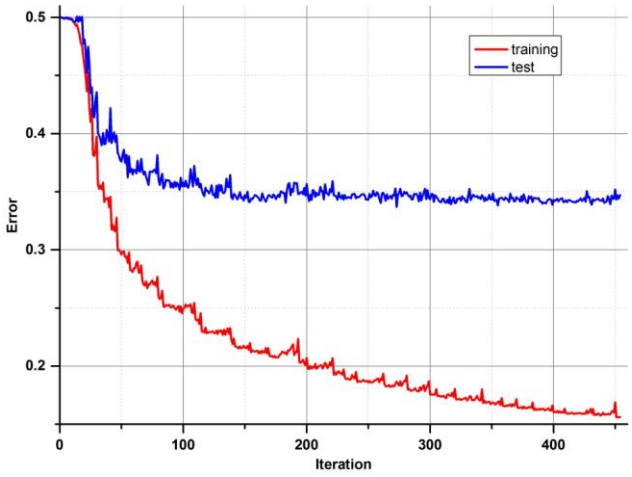

Figure 6. Example of error minimizing during training process.

Deleted: 5

3.2.1.2. Implementation of ANN for BARDet

Formatted: Indent: Hanging: 1,14 cm, Outline numbered + Level: 4 + Numbering Style: 1, 2, 3, … + Start at: 1 + Alignment: Left + Aligned at: 4,95 cm + Indent at: 3,05 cm

There are statistical commercial software packages available that provide ANN modules as one of the methods to analyze the data. It is worthwhile noting that customized software was developed for this research. This approach helped to understand ANN in depth and let to the development of software that is not only responsible for data pre-processing and network training, but also (mainly) for solving a real time classification problem.

Ruske et al. in their studies (Ruske et al., 2017) compared various algorithms to analyze single particle data and noted that ANN requires much more user input. However, we present the method to overcome this inconvenience by automatizing the process and implementing procedures, which simplifies and improves analysis.

Deleted: that

The main disadvantage of ANN is the fact that it is a parametrized algorithm. How well it works depends strictly on a proper choice of the best possible factors, which may be different for each problem. There are two types of factors that influence the ANN outcome. The first one corresponds to the architecture of ANN which comprises: number of layers, neurons and activation function parameter. The second one determines the learning process: momentum and learning rate. The last one can be tuned during the learning process to make it much faster. The “bold driver” procedure was chosen for that purpose. It continuously increases the learning rate unless an error is higher from that before the change. If it is, the algorithm radically decreases the learning rate and obtains weights from the last step again. Teaching ANN is a stochastic process caused by using randomly chosen initial weights. It was found that the best procedure for this investigation would be to make all optimization processes that way. Therefore, parameters of ANN, responsible both for structure and learning process, are randomly selected until the desired result is reached. In fact, the calculations are done automatically and simultaneously for several models due to multi core oriented software. The benefits of this approach are: time saving and high effectiveness of finding the best model. The last one is especially important, because the goal is to create a model that produces the best results, which doesn’t necessary mean creating a more complicated network (more neurons or

layers).

3.2.2. Model evaluation

The main goal of the analysis described in this paper is to find a solution to the bio-aerosol classification problem. When a training process ends, a final model is created: a network, which has a unique structure and a set of weights. One can create many of them and make a comparison only by a final error. It is not the best solution, because the goal is to distinguish patterns in data consistently, not to produce a network with a minimal error. That is why there is a need to make a final analysis of the results and evaluate the model in accordance with the best classification performance.

The standard method for visualization of results is a confusion matrix which will be necessary for Receiver Operating Characteristics (ROC) analysis (Fawcett, 2006). It simply shows what fraction of population for each class is predicted correctly or not. Each element from the data set is assigned to one of the following fits of the confusion matrix: True Positive (TP), True Negative (TN), False Negative (FN) and False Positive (FP). If it belongs to TP and TN, it was classified correctly.

The ROC graphs are very simple, but useful tools for discovering whether a classifier is worth using or if it makes a random classification. It is based on two rates from confusion matrix: hit rate (6) and false alarm rate (7).

$$hit\ rate\ (true\ positive\ rate) = \frac{TP}{TP + FN} \quad (6)$$

$$false\ alarm\ rate\ (false\ positive\ rate) = \frac{FP}{FP + TN} \quad (7)$$

Each discrete classifier has a threshold level that assigns an element to a positive or negative class. The points of ROC graph (Figure 7) represent the classifier for many thresholds. The most desired curve reaches the highest true positive rate with the lowest false positive rate (convex line). The random classifier, in turn, has a hit rate equal to a false alarm rate despite threshold variation (diagonal line). To identify ROC analysis with one coefficient, the area under the curve (AUC) may be used. The higher value of AUC results in better performance (0.5-means random, 1-excellent).

Formatted: Indent: Hanging: 0,89 cm, Outline numbered + Level: 3 + Numbering Style: 1, 2, 3, … + Start at: 1 + Alignment: Left + Aligned at: 3,43 cm + Indent at: 2,16 cm

Deleted: increments one of the fields

Deleted: (Table 3)

Deleted: a diagonal (

Deleted: ,

Deleted:)

Deleted: ¶
Table 3. Structure of confusion matrix.¶
¶

Deleted: 6

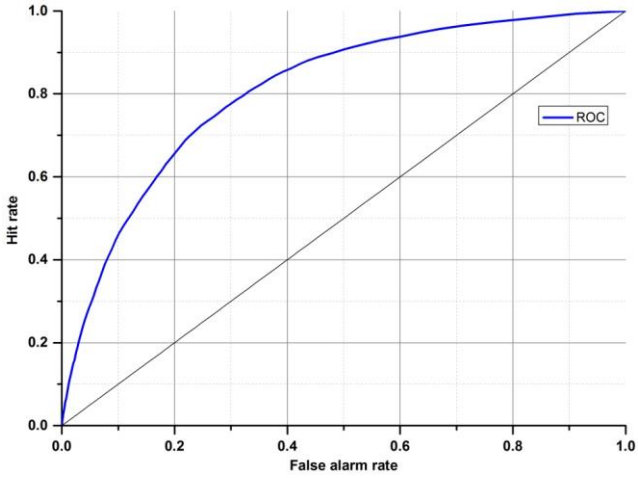

406

407 Figure 7. ROC graph with an example of classifier (blue).

408 The confusion matrix and ROC analysis described above were defined for two class problems
409 (positive, negative). There is a straightforward way to expand it for the multi-class problem. One
410 needs to take a desired class versus all other classes. Then there is a possibility to compare how good
411 the classifier for specific classes within one model is.

412 4. **Results**

413 **4.2. ANN performance**

414 The first attempts were made to distinguish all substances using only one neural network model.
415 The tests revealed that it is impossible due to the huge number of samples (48 aerosols) and only a
416 few of them presented significantly different fluorescence spectra which allow accurate
417 characterization. The remaining substances are then misclassified. Therefore, we decided to use a
418 more practical approach to this problem, which would be to create several groups (considering
419 information about aerosols), but we did not want to make any classes *a priori*. Although the
420 demonstrated ANN type needs a training, which requires a set of known classes, further tests
421 showed that there is a possibility to find similarities between substances through the analysis of
422 confusion matrices. It was achieved after many trials of matching substances, which were not well
423 separated, into new groups and checking if they are good enough on ROC graphs. Consequently, this
424 procedure was also applied to those new groups.

425

426 All examples demonstrated below were calculated on the test data sets, not training data. In the
427 first presented network (Figure 8), which try to classify all of 48 substances (group 0), four aerosols
428 reached very high accuracy of separation (AUC>0,9). The best separation was achieved for
429 fluorescent microspheres (FM7). In this case 98.5% of all FM7 particles were correctly classified.
430 Similarly, an efficient separation was achieved for riboflavin (Rib), NT (Talc) and LCB (*Lactobacillus*
431 *bulgaricus*). The remaining aerosols were divided into 3 separate groups that gather the most similar
432 substances (group 1-3) (Table 3). The subsequent groups up to 21 represent individual ANNs leading
433 to the final classification of the aerosol. In practice separation is done not by one confusion matrix
434 (ANN) but by all of them in sequence (22 ANN's combined in a decision tree). For example, if ANN

Deleted: 6

Formatted: Indent: Hanging: 0,63 cm, Outline numbered + Level: 1 + Numbering Style: 1, 2, 3, … + Start at: 3 + Alignment: Left + Aligned at: 0,63 cm + Indent at: 0,63 cm

Formatted: Indent: Hanging: 0,76 cm, Outline numbered + Level: 2 + Numbering Style: 1, 2, 3, … + Start at: 2 + Alignment: Left + Aligned at: 2,03 cm + Indent at: 1,4 cm

Deleted: F

Deleted: .

Deleted: A

Deleted: 7

Deleted: Very high separation

Deleted: efficiency

Deleted: 4

classifies unknown substance into any of 22 groups it means that decision process is not ended but from that moment another ANN classifies this substance. However, each new ANN is trained using only subsection of the data excluding the data from other groups.

Table 3. Exemplary confusion matrix of all aerosols classified by the first ANN.

		predicted						
		FM7	Rib	NT	LCB	group 3	group 1	group 2
true	FM7	98.5	0	0	0.3	0.1	0	1.1
	Rib	0.1	91	0.5	3.1	1.2	0.6	3.4
	NT	0	0.1	86.5	0	9.3	0.3	3.8
	LCB	1	1.6	0.6	72.7	3.9	10.7	9.5
	group 3	0	0.7	6.6	0.6	63.3	12	16.8
	group 1	0.2	1	1	7.9	12.5	61.6	15.8
	group 2	0.1	1.2	3.8	6.6	17.6	13.2	57.4

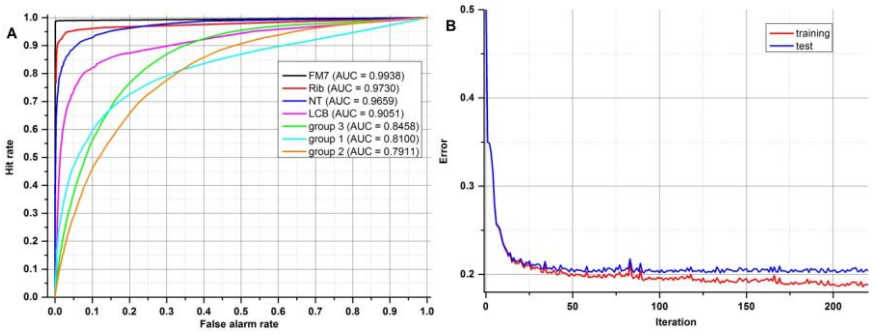

Figure 8. (A) ROC and (B) error progress of ANN that classifies all samples.

Table 4 and Figure 9 show results achieved for two substances that have very similar spectrum and calculated AUCs are not much higher than in a random classifier. This example clearly shows why we are not always able to classify each one particle of aerosol with 100% accuracy. However, just a representative number (several dozen) of measured particles (cloud) allows the proper prediction of aerosol types within a few seconds. This is easy to observe during real time detection, because counts allocated in confusion matrix tend to reach a stable state quite quickly.

		predicted	
		BWF	Cel
true	BWF	54.8	45.2
	Cel	45.6	54.4

Table 4. Confusion matrix of two substances that have very similar spectra.

Deleted: ¶
¶
¶
Deleted: 4
Deleted: C
Deleted: 7
Deleted: 5
Deleted: 8
Deleted: ¶

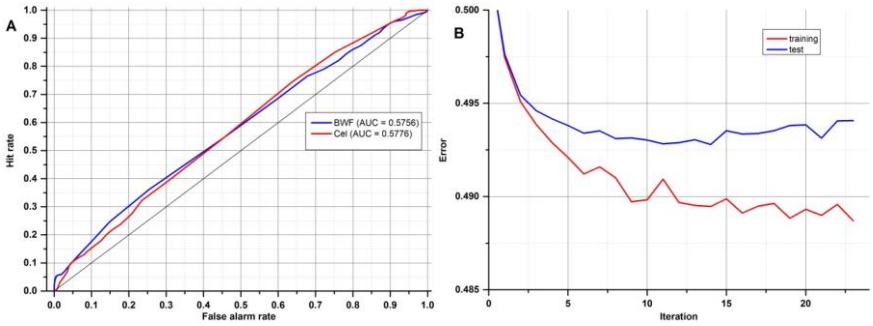

Figure 9. ROC (A) and error progress (B) of ANN that classifies two very similar samples.

4.3. Classification tree

Finally, to achieve the best possible classification, the decision tree was created (Figure 10). It comprises not one, but 22 models. It is difficult to present confusion matrices and ROC graphs for all neural networks in this paper; therefore, only the most interesting one has been discussed. Here, each node represents a network that classifies a group of aerosols. The aerosols on the left side of the diagram show the most distinct differences, thus they are easy to classify (Level 0). In the right direction (Level 1-5) this task is much more demanding due to similar spectrum and the separation is less probable in accordance to single particles, although it is still very useful from a practical point of view for aerosol cloud discrimination.

Deleted: 8

Formatted: Indent: Hanging: 0,76 cm, Outline numbered + Level: 2 + Numbering Style: 1, 2, 3, … + Start at: 2 + Alignment: Left + Aligned at: 2,03 cm + Indent at: 1,4 cm

Deleted: 9

Deleted: , so

Deleted: still

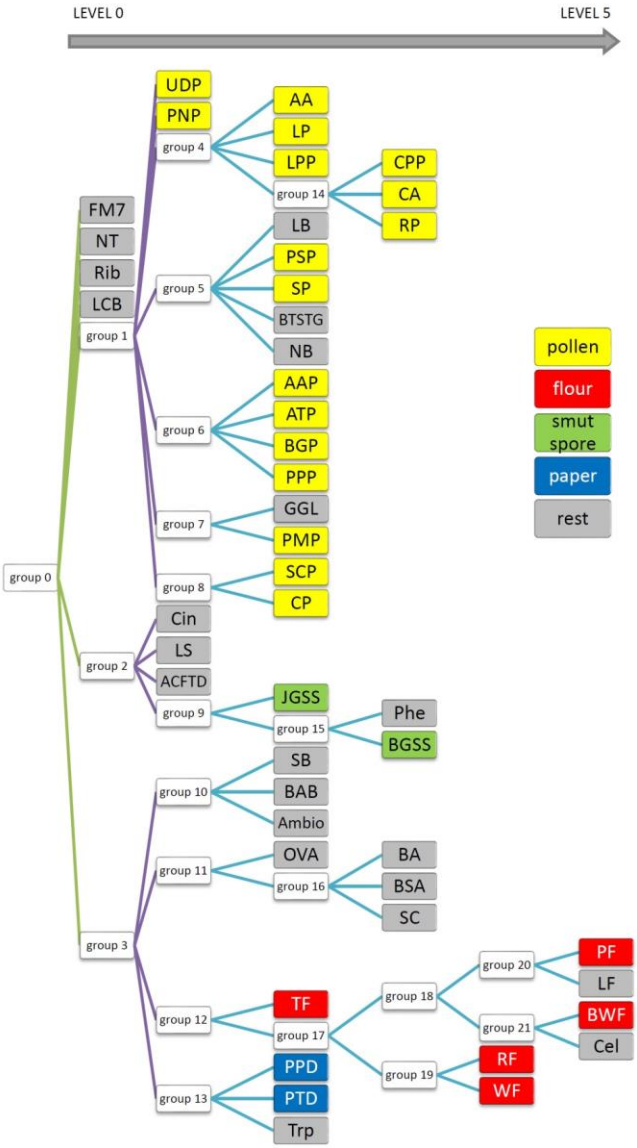

Figure 10. Decision tree consists of 22 ANN separating 48 substances.

Deleted: 9

At first glance one could see that FM7 and Rib are very well recognized, but that was expected, because these are standards of fluorescence. Surprisingly, NT and LCB aerosols were also separated from the others (Level 0 network). Further analysis of the tree structure identifies a correlation between samples and their real categories, especially it is noticeable for Pollens, which are allocated on a separate branch of that tree and all stems from group 1. Most of them were classified on the third level. Interestingly all grass pollens (AAP, ATP, BGP, PPP) belong to the same group 6. Similarly,

both *Lycopodium* pollens from different regions of the word show close correlation, however *Abies alba*, which is a tree, was classified to the same group. Flours, Smut Spores and Papers are dispersed between different levels, but particular groups belong to the same branch of the tree. However, some of samples, are scattered on the whole tree area and do not correspond to any group.

It should be noted that the result is a system of 22 ANNs that works simultaneously. In comparison to the training process, which is rather time consuming and has to be empirically optimized, this cluster of learned ANN's delivers high performance. Input data is processed by a single ANN in milliseconds. This performance makes neural network a great tool as a splitting node in the classification tree. Comparing to our previous results, where Principal Component Analysis was applied to analyze data from BARDet (Kaliszewski et al., 2016), the ANN allowed much better discrimination between various bio-aerosols.

5. Summary

In this paper the possibility of an application of the Artificial Neural Network (ANN) for a real time classification of biological aerosols was investigated. The spectral characteristics of bio-aerosols were collected using the BARDet instrument. The database consisted of 48 substances. Finally, 22 neural networks were trained and combined into a decision tree. It allowed to characterize aerosols in real time. Tests revealed that only several substances have such characteristic fluorescence spectra that allows correct classification of almost each particle. However, in all other cases the system was able to recognize a particular aerosol accurately with no mistake, but a representative number of several dozens of particles in a cloud was necessary. Further approximation was based on decision tree analysis where each node corresponded to a separate learned ANN. The best sets of ANN's for each group of similar aerosols were discovered utilizing confusion matrices and ROC analysis. Our intentions were to make a complete system which detects and classifies substances without creating groups *a priori*. This attitude helped to create a powerful analytical tool that works automatically and the results of classification are immediately available on the operator's screen.

This study proved that it is possible to create a tool for a highly effective analysis of bio-aerosols using multiple ANNs combined into decision tree. Our approach allowed to automate and speed up an analysis, which reduced time and the amount of needed computing power. In a future study the database will be extended to obtain possibly vast variety of samples including atmospherically relevant bacteria and fungi. In the next step the actual performance of the system will be determined under real environmental conditions.

Data availability: The experimental aerosol data can be provided upon request. The software for automatic data analysis cannot be commonly provided at this moment since it is a subject of negotiations with a company.

Acknowledgments

Presented work was supported by grant from The National Centre of Research and Development (Poland), project: "Mobile laboratory for environmental sampling and identification of biological threats" (O ROB 0031 01/ID/31/1).

Deleted: very

Formatted: Indent: Hanging: 0,63 cm, Outline numbered + Level: 1 + Numbering Style: 1, 2, 3, … + Start at: 3 + Alignment: Left + Aligned at: 0,63 cm + Indent at: 0,63 cm

Deleted: Finally, t

Deleted: a large data set of 114 799 samples (particle characteristics)

Deleted: It ensured that application of the ANN was fully justified.

Deleted: we

Deleted: 22

Deleted: neural networks

Deleted: them

Deleted: , which was laborious and time consuming

Deleted: However, trained ANN's

Deleted:

Deleted: d

Deleted: single particles

Deleted:

Formatted: Not Highlight

Deleted: automation

Deleted: of

Deleted: we will extend

Deleted: Finally

Deleted: What is important

Deleted: ,

Formatted: Font: (Default) Calibri, 11 pt, Font color: Black

References

Agranovski, V., Ristovski, Z., Hargreaves, M., Blackall, P. J. and Morawska, L.: Performance evaluation of the UVAPS: Influence of physiological age of airborne bacteria and bacterial stress, J. Aerosol Sci., 34(12), 1711–1727, doi:10.1016/S0021-8502(03)00191-5, 2003.

Antowiak, M. and Chałasińska-Macukow, K. C. H. a: Fingerprint identification by using artificial neural network with optical wavelet preprocessing, , 11(4), 327–337, 2003.

Bhangar, S., Huffman, J. A. and Nazaroff, W. W.: Size-resolved fluorescent biological aerosol particle concentrations and occupant emissions in a university classroom, Indoor Air, 24(6), 604–617, doi:10.1111/ina.12111, 2014.

Bishop, C. M.: Neural Networks for Pattern Recognition, Oxford University Press, Inc., New York, NY, USA., 1995.

Blais-Lecours, P., Perrott, P. and Duchaine, C.: Non-culturable bioaerosols in indoor settings: Impact on health and molecular approaches for detection, Atmos. Environ., 110, 45–53, doi:10.1016/j.atmosenv.2015.03.039, 2015.

Borecki, M., Korwin-Pawlowski, M. L. and Beblowska, M.: A Method of Examination of Liquids by Neural Network Analysis of Reflectometric and Transmission Time Domain Data From Optical Capillaries and Fibers, IEEE Sens. J., 8(7), 1208–1214, doi:10.1109/JSEN.2008.926182, 2008.

Choi, K., Ha, Y., Lee, H. K. and Lee, J.: Development of a biological aerosol detector using laser-induced fluorescence and a particle collection system, Instrum. Sci. Technol., 42(2), 200–214, doi:10.1080/10739149.2013.855639, 2014.

Davidson, C. I., Phalen, R. F. and Solomon, P. A.: Airborne particulate matter and human health: A review, Aerosol Sci. Technol., 39(8), 737–749, doi:10.1080/02786820500191348, 2005.

Deguillaume, L., Leriche, M., Amato, P., Ariya, P. a., Delort, A. M., Pöschl, U., Chaumerliac, N., Bauer, H., Flossmann, a. I. and Morris, C. E.: Microbiology and atmospheric processes: chemical interactions of Primary Biological Aerosols, Biogeosciences Discuss., 5(1), 841–870, doi:10.5194/bgd-5-841-2008, 2008.

Fawcett, T.: An introduction to ROC analysis, Pattern Recognit. Lett., 27(8), 861–874, doi:https://doi.org/10.1016/j.patrec.2005.10.010, 2006.

Deleted: Bibliography

Formatted: German (Germany)

589 Fennelly, M. J., Sewell, G., Prentice, M. B., O'Connor, D. J. and Sodeau, J. R.: Review: The Use
590 of Real-Time Fluorescence Instrumentation to Monitor Ambient Primary Biological Aerosol
591 Particles (PBAP), Atmosphere (Basel)., 9(1), 2018.

592 Feugnet, G., Lallier, E., Grisard, A., McIntosh, L., Hellström, J. E., Jelger, P., Laurell, F., Albano,
593 C., Kaliszewski, M., Wlodarski, M., Mlynczak, J., Kwasny, M., Zawadzki, Z., Mierczyk, Z.,
594 Kopczynski, K., Rostedt, A., Putkiranta, M., Marjamäki, M., Keskinen, J., Enroth, J., Janka, K.,
595 Reinivaara, R., Holma, L., Humppi, T., Battistelli, E., Iliakis, E. and Gerolimos, G.: Improved
596 laser-induced fluorescence method for bio-attack early warning detection system, in
597 Proceedings of SPIE - The International Society for Optical Engineering, vol. 7116, Thales
598 Research and Technology, France., 2008.

599 Fröhlich-Nowoisky, J., Kampf, C. J., Weber, B., Huffman, J. A., Pöhlker, C., Andreae, M. O.,
600 Lang-Yona, N., Burrows, S. M., Gunthe, S. S., Elbert, W., Su, H., Hoor, P., Thines, E.,
601 Hoffmann, T., Després, V. R. and Pöschl, U.: Bioaerosols in the Earth system: Climate, health,
602 and ecosystem interactions, Atmos. Res., 182, 346–376,
603 doi:10.1016/j.atmosres.2016.07.018, 2016.

604 Fuzzi, S., Baltensperger, U., Carslaw, K., Decesari, S., Denier Van Der Gon, H., Facchini, M. C.,
605 Fowler, D., Koren, I., Langford, B., Lohmann, U., Nemitz, E., Pandis, S., Riipinen, I., Rudich, Y.,
606 Schaap, M., Slowik, J. G., Spracklen, D. V., Vignati, E., Wild, M., Williams, M. and Gilardoni, S.:
607 Particulate matter, air quality and climate: Lessons learned and future needs, Atmos. Chem.
608 Phys., 15(14), 8217–8299, doi:10.5194/acp-15-8217-2015, 2015.

609 Gabey, A. M., Gallagher, M. W., Whitehead, J., Dorsey, J. R., Kaye, P. H. and Stanley, W. R.:
610 Measurements and comparison of primary biological aerosol above and below a tropical
611 forest canopy using a dual channel fluorescence spectrometer, Atmos. Chem. Phys., 10(10),
612 4453–4466, doi:10.5194/acp-10-4453-2010, 2010.

613 Gabey, A. M., Stanley, W. R., Gallagher, M. W. and Kaye, P. H.: The fluorescence properties
614 of aerosol larger than 0.8 μ in urban and tropical rainforest locations, Atmos. Chem. Phys.,
615 11(11), 5491–5504, doi:10.5194/acp-11-5491-2011, 2011.

616 Górny, R. L.: Filamentous microorganisms and their fragments in indoor air - A review, Ann.
617 Agric. Environ. Med., 11(2), 185–197, doi:10.1007/BF02677055, 2004.

618 Hernandez, M., Perring, A. E., McCabe, K., Kok, G., Granger, G. and Baumgardner, D.:
619 Chamber catalogues of optical and fluorescent signatures distinguish bioaerosol classes,
620 Atmos. Meas. Tech., 9(7), 3283–3292, doi:10.5194/amt-9-3283-2016, 2016.

621 Hill, S. C., Pinnick, R. G., Niles, S., Pan, Y.-L., Holler, S., Chang, R. K., Bottinger, J., Chen, B. T.,
622 Orr, C.-S. and Feather, G.: Realtime Measurement of Fluorescence Spectra from Single

623 Airborne Biological Particles, F. Anal. Chem. Technol., 3(4–5), 221–239,
624 doi:10.1002/(SICI)1520-6521(1999)3:4/5<221::AID-FACT2>3.3.CO;2-Z, 1999.

625 Huffman, J. A., Treutlein, B. and Pöschl, U.: Fluorescent biological aerosol particle
626 concentrations and size distributions measured with an Ultraviolet Aerodynamic Particle
627 Sizer (UV-APS) in Central Europe, Atmos. Chem. Phys., 10(7), 3215–3233, doi:10.5194/acp-
628 10-3215-2010, 2010.

629 Kaliszewski, M., Trafny, E. A., Lewandowski, R., Włodarski, M., Bombalska, A., Kopczyński, K.,
630 Antos-Bielska, M., Szpakowska, M., Młyńczak, J., Mularczyk-Oliwa, M. and Kwaśny, M.: A
631 new approach to UVAPS data analysis towards detection of biological aerosol, J. Aerosol Sci.,
632 58, 148–157, doi:https://doi.org/10.1016/j.jaerosci.2013.01.007, 2013.

633 Kaliszewski, M., Włodarski, M., Młyńczak, J., Leśkiewicz, M., Bombalska, A., Mularczyk-Oliwa,
634 M., Kwaśny, M., Buliński, D. and Kopczyński, K.: A new real-time bio-aerosol fluorescence
635 detector based on semiconductor CW excitation UV laser, J. Aerosol Sci., 100, 14–25,
636 doi:10.1016/j.jaerosci.2016.05.004, 2016.

637 Kohlus, R. and Bottlinger, M.: Particle Shape Analysis as an example of knowledge extraction
638 by neural nets, Part. Part. Syst. Charact., 10(5), 275–278, doi:10.1002/ppsc.19930100511,
639 1993.

640 Lakowicz, J. R.: Principles of Fluorescence Spectroscopy, Second., Kluwer Academic/Plenum
641 Publishers., 1999.

642 Lee, B. U., Jung, J. H., Yun, S. H., Hwang, G. B. and Bae, G. N.: Application of UVAPS to real-
643 time detection of inactivation of fungal bioaerosols due to thermal energy, J. Aerosol Sci.,
644 41(7), 694–701, doi:https://doi.org/10.1016/j.jaerosci.2010.04.003, 2010.

645 Leśkiewicz, M., Kaliszewski, M., Mierczyk, Z. and Włodarski, M.: Comparison of Principal
646 Component Analysis and Linear Discriminant Analysis applied to classification of excitation-
647 emission matrices of the selected biological material, Biul. Wojsk. Akad. Tech., 65(1), 15–31,
648 doi:10.5604/12345865.1197960, 2016.

649 Lim, D. V., Simpson, J. M., Kearns, E. A. and Kramer, M. F.: Current and developing
650 technologies for monitoring agents of bioterrorism and biowarfare, Clin. Microbiol. Rev.,
651 18(4), 583–607, doi:10.1128/CMR.18.4.583-607.2005, 2005.

652 Mauderly, J. L. and Chow, J. C.: Health effects of organic aerosols., 2008.

653 Miaskiewicz-Peska, E. and Lebkowska, M.: Comparison of aerosol and bioaerosol collection

654 on air filters, Aerobiologia (Bologna)., 28(2), 185–193, doi:10.1007/s10453-011-9223-1,
655 2012.

656 Michaels, R. A.: Environmental Moisture, Molds, and Asthma—Emerging Fungal Risks in the
657 Context of Climate Change, Environ. Claims J., 29(3), 171–193,
658 doi:10.1080/10406026.2017.1345521, 2017.

659 Pan, Y. Le, Hill, S. C., Pinnick, R. G., House, J. M., Flagan, R. C. and Chang, R. K.: Dual-
660 excitation-wavelength fluorescence spectra and elastic scattering for differentiation of single
661 airborne pollen and fungal particles, Atmos. Environ., 45(8), 1555–1563,
662 doi:10.1016/j.atmosenv.2010.12.042, 2011.

663 Pan, Y. Le, Huang, H. and Chang, R. K.: Clustered and integrated fluorescence spectra from
664 single atmospheric aerosol particles excited by a 263- and 351-nm laser at New Haven, CT,
665 and Adelphi, MD, J. Quant. Spectrosc. Radiat. Transf., 113(17), 2213–2221,
666 doi:10.1016/j.jqsrt.2012.07.028, 2012.

667 Pinnick, R. G., Hill, S. C., Pan, Y. Le and Chang, R. K.: Fluorescence spectra of atmospheric
668 aerosol at Adelphi, Maryland, USA: Measurement and classification of single particles
669 containing organic carbon, Atmos. Environ., 38(11), 1657–1672,
670 doi:10.1016/j.atmosenv.2003.11.017, 2004.

671 Pöhlker, C., Huffman, J. A. and Pöschl, U.: Autofluorescence of atmospheric bioaerosols:
672 Spectral fingerprints and taxonomic trends of pollen, Atmos. Meas. Tech., 6(12), 3369–3392,
673 doi:10.5194/amt-6-3369-2013, 2013.

674 Pope III, C. A. and Dockery, D. W.: 2006 Critical Review: Health Effects of Fine Particulate Air
675 Pollution: Lines That Connect, J. Air Waste Manag. Assoc., 56(6), 709–742,
676 doi:10.1080/10473289.2006.10464485, 2006.

677 Pósfai, M. and Buseck, P. R.: Nature and Climate Effects of Individual Tropospheric Aerosol
678 Particles, Annu. Rev. Earth Planet. Sci., 38(1), 17–43,
679 doi:10.1146/annurev.earth.031208.100032, 2010.

680 Purnomo, H. D., Hartomo, K. D. and Prasetyo, S. Y. J.: Artificial Neural Network for Monthly
681 Rainfall Rate Prediction, IOP Conf. Ser. Mater. Sci. Eng., 180(1), 12057, 2017.

682 Ruske, S., Topping, D. O., Foot, V. E., Kaye, P. H., Stanley, W. R., Crawford, I., Morse, A. P. and
683 Gallagher, M. W.: Evaluation of machine learning algorithms for classification of primary
684 biological aerosol using a new UV-LIF spectrometer, Atmos. Meas. Tech., 10(2), 695–708,
685 doi:10.5194/amt-10-695-2017, 2017.

686 Shiraiwa, M., Selzle, K. and Pöschl, U.: Hazardous components and health effects of
687 atmospheric aerosol particles: reactive oxygen species, soot, polycyclic aromatic compounds
688 and allergenic proteins, Free Radic. Res., 46(8), 927–939,
689 doi:10.3109/10715762.2012.663084, 2012.

690 Taketani, F., Kanaya, Y., Nakamura, T., Koizumi, K., Moteki, N. and Takegawa, N.:
691 Measurement of fluorescence spectra from atmospheric single submicron particle using
692 laser-induced fluorescence technique, J. Aerosol Sci., 58, 1–8,
693 doi:https://doi.org/10.1016/j.jaerosci.2012.12.002, 2013.

694 Trafny, E. A., Lewandowski, R., Stępińska, M. and Kaliszewski, M.: Biological threat detection
695 in the air and on the surface: How to define the risk, Arch. Immunol. Ther. Exp. (Warsz).,
696 62(4), 253–261, doi:10.1007/s00005-014-0296-8, 2014.

697